Short-Path Near-Infrared Laser Detection of Environmental Gases by Wavelength-Modulation Spectroscopy

Isao Tomita

Abstract—The detection of environmental gases, $^{12}CO_2$, $^{13}CO_2$, and CH_4, using near-infrared semiconductor lasers with a short laser path length is studied by means of wavelength-modulation spectroscopy. The developed system is compact and has high sensitivity enough to detect the absorption peaks of isotopic $^{13}CO_2$ of a 3-% CO_2 gas at 2 μm with a path length of 2.4 m, where its peak size is two orders of magnitude smaller than that of the ordinary $^{12}CO_2$ peaks. In addition, the detection of $^{12}CO_2$ peaks of a 385-ppm (0.0385-%) CO_2 gas in the air is made at 2 μm with a path length of 1.4 m. Furthermore, in pursuing the detection of an ancient environmental CH_4 gas confined to a bubble in ice at the polar regions, measurements of the absorption spectrum for a trace gas of CH_4 in a small area are attempted. For a 100-% CH_4 gas trapped in a $\sim$ 1 mm^3 glass container, the absorption peaks of CH_4 are obtained at 1.65 μm with a path length of 3 mm, and also the gas pressure is extrapolated from the measured data.

Keywords—Environmental Gases, Near-Infrared Laser Detection, Wavelength-Modulation Spectroscopy.

I. INTRODUCTION

THE detection of environmental gases, such as CO_2 and CH_4, is now attracting considerable attention in the investigation of greenhouse effects [1], [2]. In particular, the measurement of the CO_2 concentration in the atmosphere is frequently made by LIDAR (LIght Detection And Ranging) [3], which collects the back-scattering data from the target gas with a distance of kilometers by exposure with laser beams generated from high-power, sizable lasers, e.g., CO_2 and YAG lasers [4]–[8]. On the other hand, in the field of investigating ancient environmental gases, much attention has been paid to a gas trapped in the bubbles of ice at the polar regions. A conventional method for studying this uses a special chamber that collects the gas by crushing ice for a CO_2 gas [9] and by melting ice for a CH_4 gas [10]. But, in both cases, the chamber is sizable and takes considerable time to extract the gas. If the chamber is eliminated, the system will be compact. In addition, if a method to collect the data of the gas directly from the bubble is devised, the data acquisition time will be shortened. Moreover, if the system has a laser-targeting system towards the bubble, it will be a very convenient system. A detection system with those properties will be useful for on-site measurements where ice samples are obtained.

For that purpose, a compact laser-based detection system with a short laser path length is developed with

Isao Tomita is with Department of Electrical and Computer Engineering, Gifu National College of Technology, 2236-2 Kamimakuwa, Motosu, Gifu 501-0495, Japan (e-mail: itomita@gifu-nct.ac.jp).

near-infrared semiconductor lasers of 1.65 and 2 μm. The detection sensitivity is enhanced by wavelength-modulation spectroscopy (WMS) [11]–[14]. With this system, the absorption peaks of the isotopic $^{13}CO_2$ component of a 3-% CO_2 gas are detected at 2 μm with a path length of 2.4 m, where its peak amplitude is two orders of magnitude smaller than that of the ordinary $^{12}CO_2$ component. Also, the absorption spectrum of the $^{12}CO_2$ component of a 385-ppm (0.0385-%) CO_2 gas is measured at 2 μm in the air with a path length of 1.4 m. Furthermore, the absorption peaks of a trace gas of pure CH_4 in a minuscule area ($\sim$ 1 mm^3) are obtained at 1.65 μm with a path length of 3 mm. The details of the constructed system are described in the next section.

II. DEVELOPED SYSTEM

A schematic diagram of the developed system with WMS is depicted in Fig. 1. WMS is a method that can extract derivative signals from faint absorption peaks. To perform WMS, a sawtooth-type voltage change with a sinusoidal voltage modulation generated from a function generator is employed, where the sawtooth-type voltage change has a period of $t_0 = 0.1$ s (or a frequency of $f_0 = 10$ Hz) and the sinusoidal voltage modulation has a period of $t = 1.0 \times 10^{-4}$ s (or a frequency of $f = 10$ kHz). f is set at 10 kHz so that the derivative signals can be obtained clearly. This voltage modulation is then sent to a laser diode (LD) driver to convert it into a modulated current. This modulated current is injected into a 2-μm InGaAs LD [15]–[17] with a maximum power of 2 mW to transfer the same modulation to the laser beam.
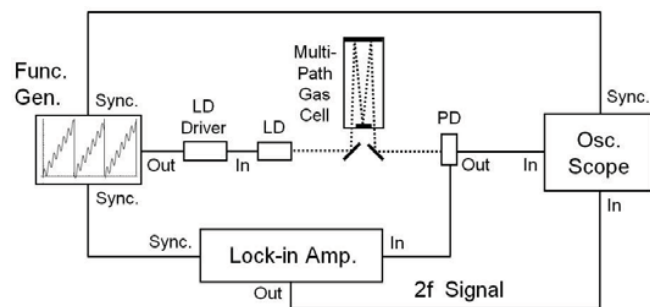

Fig. 1 Experimental setup.

The sawtooth-type change with $f_0 = 10$ Hz in the LD injection current works as wavelength-sweeping because it causes an LD refractive-index change and thus a wavelength

TABLE I
PEAK POSITIONS IN WAVELENGTH FOR $^{13}CO_2$ AND $^{12}CO_2$
AT AROUND 2.006 μm.

No.	Molecule	λ [μm]	κ [cm^{-1}]	Spectral strength [a.u.]
1	$^{12}CO_2$	2.0063683	4984.129845	3.158×10^{-23}
2	$^{12}CO_2$	2.0062970	4984.306792	2.962×10^{-23}
3	$^{12}CO_2$	2.0062085	4984.526883	1.033×10^{-21}
4	**$^{13}CO_2$**	**2.0060544**	**4984.909710**	**5.203×10^{-24}**
5	$^{12}CO_2$	2.0058833	4985.334836	2.752×10^{-23}

shift. Here, the maximum amount of the injection current determines an attainable wavelength-sweeping range ($\sim$ 1 nm).

The modulated laser beam from LD passes through a multi-path gas cell with a path length of 2.4 m and reaches an InGaAs photodiode (PD) detector. The detected signals at PD are then fed into a lock-in amplifier. This lock-in amplifier extracts the $2f$ component of the signals with low noise, which is equivalent to the 2nd *derivative* component of the signals. Finally, the extracted signals are sent to an oscilloscope to display the results every 0.1 s. In this way, faint absorption peaks are obtained as derivative signals. This is the merit of using WMS. Note that in addition to small semiconductor LD and PD, compact measurement instruments were employed here such that they were packed into a box of $450\,\text{mm} \times 160\,\text{mm} \times 380\,\text{mm}$ (roughly the size of a traveling suitcase).

III. EXPERIMENTAL RESULTS AND DISCUSSION

A. Absorption-Spectrum Measurement of CO_2

As a test gas, a 3-% CO_2 gas at 100 Torr and 25 deg C was used. This concentration is almost equal to that of a CO_2 gas in our breath exhaled to the atmosphere. Here, the composition ratio between $^{13}CO_2$ and $^{12}CO_2$ was set to be the same ratio in the air. As the rest (97 %) of the gas, it was filled with N_2.

The laser beam generated from LD was set at around 2.006 μm. For quick identification of $^{13}CO_2$ peaks, the relative peak positions of $^{13}CO_2$ to those of $^{12}CO_2$ were examined in advance by use of HITRAN [18], as shown in Table I, where λ [μm] and κ [cm^{-1}] are the laser wavelength and wavenumber, respectively. Since obtainable data in experiments are the transmission rates of a laser beam passing through the mixture of $^{12}CO_2$ and $^{13}CO_2$ with a path length of 2.4 m at 100 Torr and 25 deg C, the transmission rate was calculated at the same condition with MOLSPEC [19], which is illustrated in Fig. 2.

Next, we show experimental results: The slope of Fig. 3(a) depicts measured, bare signals at the InGaAs PD detector before the extraction of the $2f$ signals. Fig. 3(a) exhibits only a big absorption peak corresponding to No. 3 in Table I, which is the main peak at this wavelength region. The sinusoidal modulation thickens the measured curve. But when it was turned off, the other peaks than No. 3 were still obscure.

The $2f$ signals were then extracted from the above bare signals with the lock-in amplifier. In this case, all clear No. 1−5 peaks were observed, as displayed at the curve of Fig. 3(b). This No. 4 peak is the isotopic $^{13}CO_2$ peak, which is about 1/200 smaller in size than the No. 3 main peak. From the

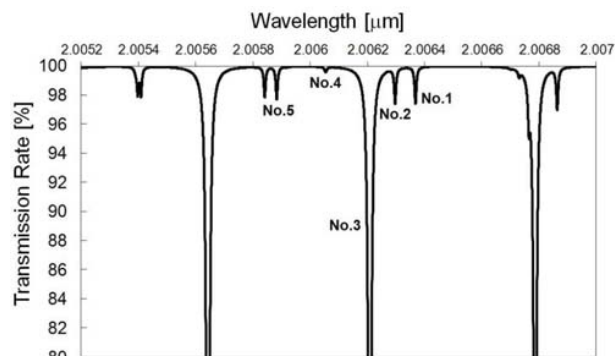Fig. 2 Calculated transmission rate for the 3-% mixture gas of $^{12}CO_2$ and $^{13}CO_2$ with a path length of 2.4 m at 100 Torr and 25 deg C.
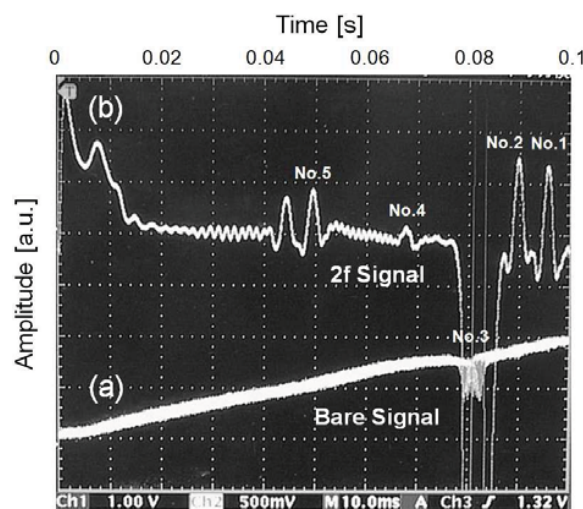

Fig. 3 (a) Measured bare signals for the mixture gas of $^{12}CO_2$ and $^{13}CO_2$, (b) $2f$ signals extracted from the measured bare signals (a).
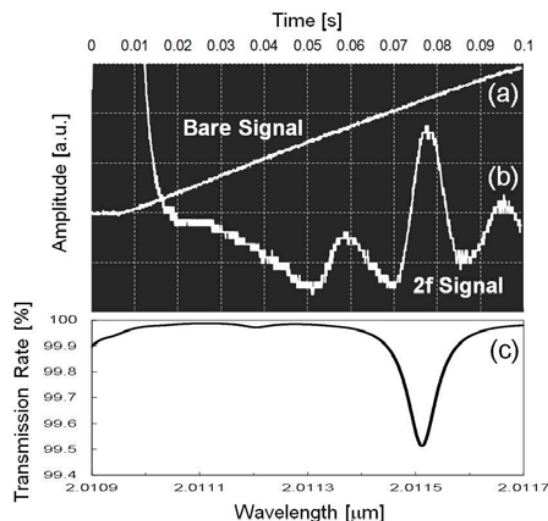

Fig. 4 (a) Measured bare signals for $^{12}CO_2$ with a concentration of 385 ppm (0.0385 %), (b) $2f$ signals extracted from the measured bare signals (a), (c) Calculated transmission rate for the 385-ppm $^{12}CO_2$ gas.

viewpoint of transmission rates, the developed system has an ability to measure absorption peaks for a transmission rate of 99.5 % (i.e., an absorption rate of 0.5 %), as seen for the No.4 peak in Fig. 2 and Fig. 3(b).

Next, shown at the slope of Fig. 4(a) are measured, bare signals at around 2.011 μm for a 385-ppm (0.0385-%) $^{12}CO_2$ gas in the air at 760 Torr and 25 deg C with a path length of 1.4 m, where the sinusoidal modulation was turned off. Although Fig. 4(a) displayed no absorption peaks, after the extraction of the $2f$ signals, a large peak was observed, as displayed at the curve of Fig. 4(b). We can confirm that this peak matches that at 2.0115 μm with a transmission rate of 99.5 % (i.e., an absorption rate of 0.5 %), as shown in Fig. 4(c) calculated by MOLSPEC.

B. Absorption-Spectrum Measurement of CH₄

Next, the absorption spectrum of a CH_4 gas in a minuscule area was measured, which could not be obtained by the ordinary wavelength-sweeping method.

As a sample to measure, having in mind investigating an ancient environmental CH_4 gas trapped in a bubble of ice at the polar regions, we prepared a small glass container enclosing the gas with an interior volume of only ~ 1 mm^3. This was made in such a way that both sides of a 1-mm-long hollow glass tube was heat-sealed at 1000 deg C with two 1-mm-thich glass caps in a pure CH_4 atmosphere at 760 Torr (Even at this high temperature, pure CH_4 was not ignited because of no oxygen). Due to this heat-sealing, as the sample was cooled down to room temperature (25 deg C), the pressure of the enclosed gas would be decreased. The value of this decreased pressure will be estimated later in this section.

To measure the absorption spectrum of the CH_4 gas effectively, the 2-μm LD was changed to a 1.65-μm LD [17], and the sample was set between the laser and the detector with a separation of 3 mm.

In addition, to check the peak positions of the CH_4 gas for easier measurements, the data of them were obtained in advance by using a much longer glass cell with the ordinary wavelength-sweeping method, where the cell contained a pure CH_4 gas with 90 Torr at 25 deg C and was set in place of the multi-path gas cell in Fig. 1. Fig. 5(a) is the target absorption peak in this case, and Fig. 5(b) is the calculated transmission rate for the 20-cm-long cell. Here, we can see that the target peak actually has two peaks at 90 Torr. Fig. 5(c) shows the measured data. From the shape of the observed peaks that fits that of the calculation, wavelength data can be precisely given to the observed peaks.

The slope of Fig. 6(a) shows measured, bare signals through the 1-mm^3 CH_4 gas in the sample after the replacement of the 20-cm-long cell, while pointing the laser beam towards the small hole of the sample filled with CH_4. But as long as the ordinary wavelength-sweeping method was used, no absorption peaks were observed, as depicted at the slope of Fig. 6(a). By the extraction of the $2f$ signals, two peaks were clearly observed, as shown at the curve of Fig. 6(b), whose peak positions fit those of Fig. 6(c) (the same one in Fig. 5(c)).

Finally, from those two observed peaks, we estimated the aforementioned decreased pressure, P, of CH_4 in the sample
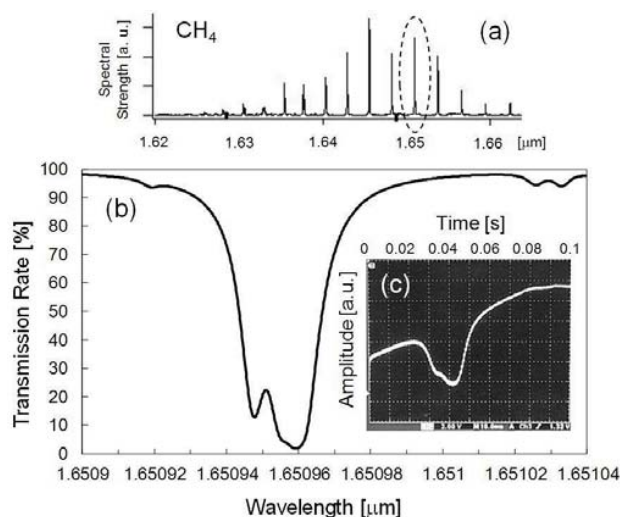

Fig. 5 (a) Target peak of CH₄, indicated by the dashed circle, (b) Calculated transmission rate for the CH₄ gas in the 20-cm-long glass cell with 90 Torr at 25 deg C, (c) Measured data of the target peak by the ordinary wavelength-sweeping method.
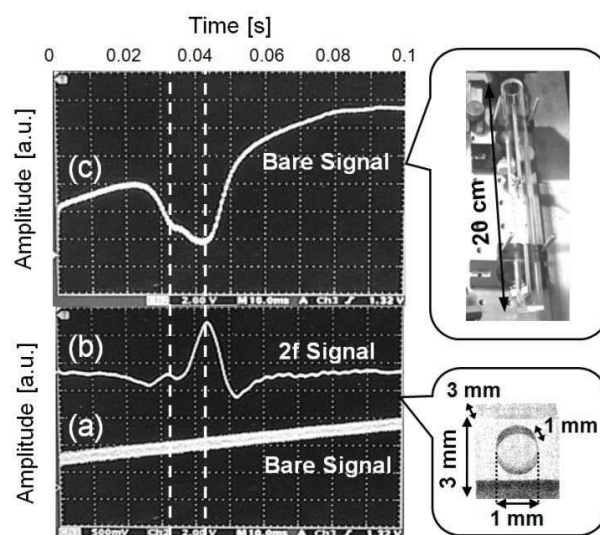

Fig. 6 (a) Measured bare signals for the CH₄ gas confined to a glass container with an interior volume of ~ 1 mm^3, (b) $2f$ signals extracted from the measured bare signals (a), (c) Measured data of the CH₄ gas in the 20-cm-long cell for comparison with (b).

that was cooled down to room temperature (25 deg C). To do this, the transmission rate through the 1-mm^3 CH_4 gas was computed in advance by changing P, as illustrated in Fig. 7. This indicates that a broad spectral line at 760 Torr becomes narrow as P decreases and that two peaks start to appear at around 200 Torr. From Fig. 7, P is estimated to be $100 < P < 200$ Torr. A more precise estimation of P can be made by Boyle-Charles' law, $PV = nRT$, where V is the gas volume, n is the number of moles of the gas, R is the gas constant (or the product of Boltzmann's constant and Avogadro's constant), and T is the absolute temperature. Using
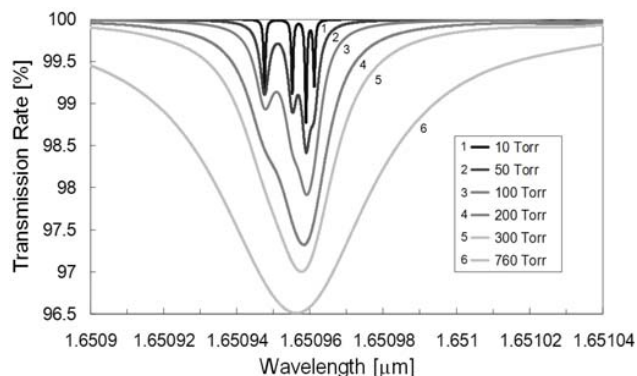
Fig. 7   Calculated transmission rate for the 1-mm^3 CH$_4$ gas at 25 deg C when the pressure is changed.

the heat-sealing temperature, 1000 deg C, at 760 Torr, we can obtain P at the room temperature, 25 deg C, for the same volume and the same number of moles as $P = 760$ Torr $\times$ $[(25 + 273.15) \text{ K}]/[(1000 + 273.15) \text{ K}] \approx 178$ Torr, which is an in-between value of 100 and 200 Torr.

IV. Summary

Constructing a compact laser-based detection system with WMS, we detected the absorption peaks of environmental gases, ^{12}CO$_2$, ^{13}CO$_2$, and CH$_4$, using near-infrared semiconductor lasers with a short path length. Here, WMS helped to find faint absorption peaks by extracting their $2f$ signals (i.e., 2nd derivative signals) with low noise. The detection sensitivity reached that for a laser transmission rate of 99.5 % (i.e., a laser absorption rate of 0.5 %). With this sensitivity, isotopic ^{13}CO$_2$ of a 3-% CO$_2$ gas was measured at 2 μm with a path length of 2.4 m. Also, the absorption peaks of ^{12}CO$_2$ in the air with a concentration of 385 ppm (0.0385 %) were obtained at 2 μm with a path length of 1.4 m. In addition, measuring the absorption spectrum of a CH$_4$ gas captured in a small area of ice-bubble size was attempted. For a pure CH$_4$ gas enclosed in a $\sim$1-mm^3 glass container, its absorption peaks were detected while pointing a 1.65-μm laser beam towards the small hole of the sample filled with CH$_4$ with a path length of 3 mm, and also its pressure was obtained from the measured data.

Acknowledgment

References

[1] J. K. Casper, *Greenhouse Gases: Worldwide Impacts*, 1st ed., New York: Facts On File, Inc., 2010.

[2] Greenhouse Gases Factsheet, Center for Sustainable Systems, University of Michigan, 2013, Pub. No. CSS05-21.

[3] G. J. Koch, B. W. Barnes, M. Petros, J. Y. Beyon, F. Amzajerdian, J. Yu, R. E. Davis, S. Ismail, S. Vay, M. J. Kavaya, and U. N. Singh, "Coherent differential absorption lidar measurements of CO$_2$," Appl. Opt. 43, 2004, pp.5092-5099.

[4] A. I. Karapuzikov, A. N. Malov, and I. V. Sherstov, "Tunable TEA CO$_2$ laser for long-range DIAL lidar," Infrared Phys. & Tech. 41, 2000, pp.77-85.

[5] A. R. Bahrampour and A. A. Askari, "Fourier-wavelet regularized deconvolution (ForWaRD) for lidar systems based on TEA-CO$_2$ laser," Opt. Comm. 257, 2006, pp.97-111.

[6] K. E. Bozier, G. N. Pearson, F. Davies, and C. G. Collier, "Evaluating the precision of a transverse excitation atmospheric based CO$_2$ Doppler lidar system with *in situ* sensors," J. Opt. A: Pure Appl. Opt. 6, 2004, pp.608-616.

[7] S. D. Mayor, D. H. Lenschow, R. L. Schwiesow, J. Mann, C. L. Frush, and M. K. Simon, "Validation of NCAR 10.6-μm CO$_2$ Doppler lidar radial velocity measurements and comparison with a 915-MHz profiler," J. Amtos. & Ocean. Tech. 14, 1997, pp.1110-1126.

[8] D. Sakaizawa, C. Nagasawa, T. Nagai, M. Abo, Y. Shibata, M. Nakazato, and T. Sakai, "Development of a 1.6 μm differential absorption lidar with a quasi-phase-matching optical parametric oscillator and photon-counting detector for the vertical CO$_2$ profile," Appl. Opt. 48, 2009, pp.748-757.

[9] R. Zumbrunn, A. Neftel, and H. Oeschger, "CO$_2$ measurements on 1-cm^3 ice samples with an IR laser spectrometer (IRLS) combined with a new dry extraction device," Earth and Planet. Sci. Lett. 60, 1982, pp.318-324.

[10] J. R. Melton, M. J. Whiticar, and P. Eby, "Stable carbon isotope ratio analyses on trace methane from ice samples," Chemical Geology 288, 2011, pp.88-96.

[11] J. A. Silver, "Frequency-modulation spectroscopy for trace species detection: theory and comparison among experimental methods," Appl. Opt. 31, 1992, pp.707-717.

[12] H. Li, G. B. Rieker, X. Liu, J. B. Jeffries, and R. K. Hanson, "Extension of wavelength-modulation spectroscopy to large modulation depth for diode laser absorption measurements in high-pressure gases," Appl. Opt. 45, 2006, pp.1052-1061.

[13] G. B. Rieker, J. B. Jeffries, and R. K. Hanson, "Calibration-free wavelength-modulation spectroscopy for measurements of gas temperature and concentration in harsh environments," Appl. Opt. 48, 2009, pp.5546-5560.

[14] K. Tanaka and K. Tonokura, "Sensitive measurements of stable carbon isotopes of CO$_2$ with wavelength modulation spectroscopy near 2 μm," Appl. Phys. B 105, 2011, pp.463-469. A sizable multi-path gas cell with a path length of 29.9 m is used for high-precision measurements.

[15] M. Oishi, M. Yamamoto, and K. Kasaya, "2.0-μm single-mode operation of InGaAs-InGaAsP distributed-feedback buried-heterostructure quantum-well lasers," IEEE Photon. Tech. Lett. 9, 1997, pp.431-433.

[16] M. Mitsuhara, M. Ogasawara, M. Oishi, H. Sugiura, and K. Kasaya, "2.05-μm wavelength InGaAs-InGaAs distributed-feedback multiquantum-well lasers with 10-mW output power," IEEE Photon. Tech. Lett. 11, 1999, pp.33-35.

[17] The products of NTT Electronics Co. The semiconductor laser diodes used in the experiments were all obtained at http://www.ntt-electronics.com/en/products/photonics/gas_sensing.html

[18] The HITRAN database. http://www.cfa.harvard.edu/hitran/

[19] MOLSPEC. This software computes the transmission rate of a laser beam passing through a selected gas with a selected laser wavelength, path length, pressure, and temperature. http://www.lasercomponents.com/us/news/molspec-v-industrial/